Tribology International 88 (2015) 317–326

Contents lists available at ScienceDirect

Tribology International

journal homepage: www.elsevier.com/locate/triboint

Gearbox power loss. Part III: Application to a parallel axis and a planetary gearbox

Carlos M.C.G. Fernandes [a,*], Pedro M.T. Marques [a], Ramiro C. Martins [a], Jorge H.O. Seabra [b]

[a] INEGI, Universidade do Porto, Campus FEUP, Rua Dr. Roberto Frias 400, 4200-465 Porto, Portugal
[b] FEUP, Universidade do Porto, Rua Dr. Roberto Frias s/n, 4200-465 Porto, Portugal

ARTICLE INFO

Article history:
Received 6 January 2015
Received in revised form
27 February 2015
Accepted 20 March 2015
Available online 27 March 2015

Keywords:
Gearboxes
Power loss
Wind turbine gear oils

ABSTRACT

In the third part of this work, the rolling bearing torque loss model, the lubricant factor extracted from the FZG tests with wind turbine gear oils and the loss factor for helical gears, developed in Part I and Part II of this work, will be applied to predict the power loss in a parallel axis and a planetary gearbox. The numerical results obtained are compared with those from experimental tests.

1. Introduction

In the first part, thrust roller and ball bearings were tested for power loss in a modified four ball machine using different ISO VG 320 wind turbine gear oils (a mineral (MINR), a poly-alpha-olephin (PAOR), a mineral with PAMA viscosity modifier (MINE) and a poly-alkyleneglycol (PAGD)). The coefficient of friction in the rolling bearings was determined, allowing a better correlation between the numerical and measured torque loss. The model for the friction power loss in the gear meshing was also calibrated. In the second part of this work the lubricant factor (X_L) that is used to adapt the classic gear mesh coefficient of friction formula originally proposed by Schlenk et al. [1] was obtained for four different wind turbine gear oils after some experiments with helical and spur gears in an FZG test rig.

The aim of this third part is to apply the models developed in part I [2] and part II [3] of this work in order to predict, as accurately as possible, the gearbox power loss.

2. Gearbox test rig

The gearbox test rig (Fig. 1) follows the principle of recirculating power. This test rig allows the testing of gearboxes of different size and type, given that they fit within the dimensional constraints and allow for reducer/multiplier operation. Two gearboxes are used, one as speed multiplier and the other as speed reducer, in order to close the circulating power loop. This test rig allows input speeds from 100 to 1900 rpm and input torques from 100 to 1300 N m. The gearbox oil sump temperature is set free.

The gearbox test rig allows monitoring and recording several operating parameters, namely input and output torque/speed of the test gearbox; room temperature; oil sump temperature in the test gearbox in two locations; external wall temperature of the housing on both test and slave gearboxes in various points.

Industrial grade 3 wire *Pt*100 RTD's and Type K thermocouples were used to monitor the temperatures in these points.

3. Parallel axis gearbox

In previous works [4] the authors have studied the power loss behaviour of a parallel axis gearbox. This time, the numerical results are re-evaluated taking into account the coefficient of friction derived from the FZG tests and the modifications to the rolling bearings power loss model, reported in parts I and II of this work.

Fig. 2 shows a schematic view of the test gearbox. This gearbox has three shafts where five gears are mounted. The gears in the middle shaft are keyed while the gears on the first and third shafts are mounted over needle bearings. All shafts are supported by ball or roller bearings. The test gearbox allows the selection of two different kinematic relations. All tests were conducted with the test gearbox working as speed multiplier ($u \approx 2.3$).

Abbreviations: TRB, tapper roller bearing; DGBB, deep groove ball bearing; NRB, needle roller bearing; N.A., not available; N.O., not operating; N.E., non-existent

* Corresponding author.
E-mail address: cfernandes@inegi.up.pt (C.M.C.G. Fernandes).

http://dx.doi.org/10.1016/j.triboint.2015.03.029
0301-679X/

Notation and Units

a	axis distance (mm)
b	tooth face width (mm)
d_{sh}	shaft seal diameter (mm)
F_{bt}	tangential force on the base plane (N)
m	module (mm)
M_t	bearing friction torque (N mm)
M'_{rr}	rolling friction torque (N mm)
M_{sl}	sliding friction torque (N mm)
M_{drag}	friction torque of drag losses (N mm)
M_{seal}	friction torque of seals (N mm)
n_p	number of planets (–)
P_{IN}	mesh input power (W)
P^g_{IN}	gearbox input power (W)
P_V	model total power loss (W)
P_{VL}	rolling bearings power loss (W)
P_{VZ0}	no-load gears power loss (W)
P_{VZP}	meshing gears power loss (W)
P_{VD}	seals power loss (W)
Q	heat lost by dissipation (W)
R_a	arithmetic average roughness of pinion and gear (μm)
T_{oil}	oil sump temperature (°C)
T_{room}	room temperature (°C)
u	gear ratio (z_2/z_1) (–)
v_t	pitch line velocity (m/s)
x	addendum modification (–)
XL	lubricant parameter (–)
z	number of teeth (–)
α	pressure angle (deg)
$\alpha \cdot A$	Global heat transfer coefficient (W/K)
β	helix angle (deg)
ν_{oil}	oil kinematic viscosity at operating oil sump temperature (mm^2/s)
$\Delta T_{or} =$	$T_{oil} - T_{room}$ deg
$\Delta T_{ow} =$	$T_{oil} - T_{wall}$ deg
ϕ_{bl}	sliding friction torque weighting factor (–)
ϕ_{ish}	inlet shear heating reduction factor (–)
ϕ_{rs}	kinematic replenishment/starvation reduction factor (–)
μ_{bl}	coefficient of friction in boundary film lubrication (–)
μ_{EHD}	coefficient of friction in full film lubrication (–)
μ_{sl}	sliding coefficient of friction (–)

The transfer gearbox is filled with 2 l of a wind turbine gear oil with the physical and chemical properties described in the first part of the work [2].

Table 1 displays the main geometric properties of the gears used in the test gearbox. Table 2 shows information about the rolling bearings installed in the test gearbox.

Table 3 shows the test sequence and imposed input speed and torques.

3.1. Experimental results

Fig. 3 shows the experimental results in terms of stabilized operating temperatures. These results clearly indicate that usually PAGD promotes the lowest power loss and MINR the highest. The test with MINR at the highest load and speed was disregarded due to expected operating temperatures well above 100 °C. PAOR and MINE performed identically, and are positioned between MINR and PAGD.

3.2. Power loss modelling

The load dependant power loss model that was used to predict the power loss generated in the parallel axis gearbox is the same that was employed to derive the gears coefficient of friction for the torque loss measurements in Part II of the current work [3]. The model will be applied considering the power loss generated in the gearbox for the tested operating conditions for rolling bearings (Appendix A), gears (Appendix B) and seals (Appendix C).

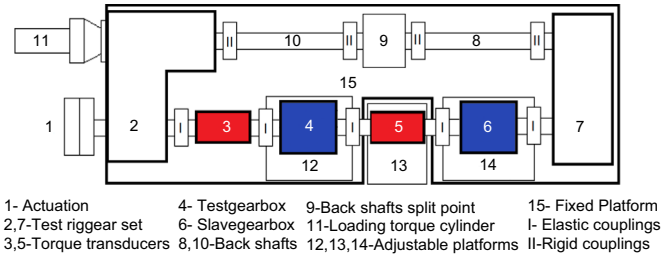

Fig. 1. Top view scheme of the gearbox test rig.

3.2.1. Gears churning loss model

For splash-lubricated gears, oil churning is a major source of power loss which is related to the fluid circulation generated by rotating gears partly immersed in a lubricant [5].

Recently, Changenet et al. [5] presented a gear churning loss model based on a dimensional analysis approach and a series of experimental tests to tune the model. This model was selected because it seeks to overcome some of the limitations of previous models [6–9] which were also based on empirical studies.

The gear churning loss model proposed by Changenet et al. [5] depends on a Reynolds number that describes the laminar–turbulent transition which was also determined after the experimental results.

The laminar–turbulent flow transition inside an oil sump lubricated gearbox is difficult to determine mainly due to the almost infinite combination of design features that exists. In previous works the authors applied this gear churning loss model to the parallel axis gearbox [10] and verified that one of the main reasons for the discrepancy between the numerical and experimental results was on the prediction of the gear churning loss. Using the Reynolds number calculated for single pinions did not allow a correct simulation of the churning losses, underestimating the churning losses importance. Based on the stabilized operating temperatures, the authors [10] found a way to determine an approximate laminar–turbulent transition point that was used to adjust the gear churning loss model.

3.3. Modelling results

Fig. 4 show the calculated power loss as well as each one of its components. For the tested operating conditions the meshing losses dominate the power loss. Depending on the oil nature, namely dynamic viscosity, the gear churning losses seem to be higher than the bearings power loss.

The measured values of power loss are presented with the power loss model predictions in Fig. 5.

At stabilized conditions the heat that is lost to the environment through the gearbox is equal to the power loss. Eq. (1) shows the relation between the stabilized operating temperature and the power that is dissipated through the gearbox:

$$Q = \alpha \cdot A \cdot \Delta T \tag{1}$$

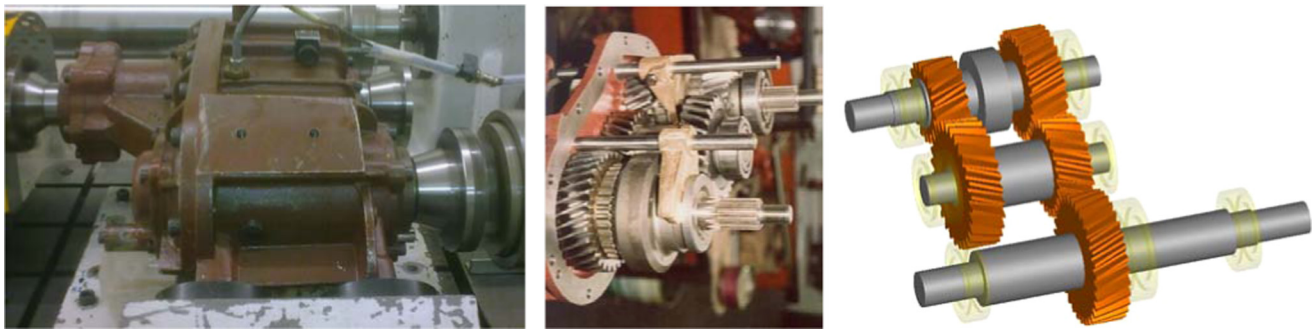

Fig. 2. Parallel axis gearbox.

Table 1
Geometrical parameters of the gears in the parallel axis gearbox.

Gears				Parameters							
				z (–)	m (mm)	a (mm)	α (G)	β (G)	b (mm)	x (–)	Ra (μm)
Parallel axis	1st stage	G1	Pinion	32	3.5	105.0	20	20	35	+0.3810	0.4
			Gear	23						+0.4150	
	2nd stage	G2	Pinion	28	4	95.0	20	20	33.5	−0.2400	0.4
			Gear	17						+0.0510	

Table 2
Rolling bearings in the test gearbox (gear oil sump lubrication).

Type	Quantity	Reference	Code
Deep groove ball	1	RMS 11	B1
Deep groove ball	1	RMS 10	B2
Deep groove ball	1	6307	B3
Tapper roller	2	32306	B4, B5
Cylindrical roller	1	NJ 309E	B6
Needle	1	K38 × 43 × 27F	–

The global heat transfer coefficient, $\alpha \cdot A$, can be used to verify the general consistency of the power loss model.

At stabilized operating conditions the global heat transfer behaviour should be more or less independent of the gear oil that is used to lubricate the gearbox (oil sump lubrication). Fig. 6 shows that $\alpha \cdot A$ follows an $\approx$ linear law which is also more or less independent of the gear oil. This shows that the model has a consistent behaviour.

Fig. 6 shows the global heat transfer coefficient calculated from the temperatures at stabilized operating conditions.

The calculated heat transfer coefficient (α), for the transfer gearbox with an area of A=0.218 m^2, is in the range 37–83 W/(m^2 K) which is in agreement with the findings published by Höhn et al. [11].

A calculation example can be found in Appendix D, for each power loss source of the transfer gearbox.

4. Planetary gearbox

The planetary speed reducer has a speed ratio of 1/4, n_{out}/n_{in}, a max input speed of 1000 rpm and an nominal output torque of 2500 Nm (Table 4). This gearbox is suited for heavy industrial applications, therefore it is capable of handling very high loads (axial and transverse) at the output shaft, which is supported by two back-to-back tapered roller bearings (Table 5). In this work, the planetary gearbox was operating in a multiplier configuration.

Fig. 7 shows the planetary gearbox installed in the gearbox test rig and a schematic.

Table 3
Sequence for the experimental tests (parallel axis gearbox).

Test Sequence (–)	Input speed (rpm)	Input torque (N m)	Input power (kW)	Total test time (h)
1	100	500	5.236	4+4
2		750	7.854	4+4
3		1000	10.472	4+4
4	200	500	10.472	4+4
5		750	15.708	4+4
6		1000	20.944	4+4
7	400	500	20.944	4+4
8		750	31.416	4+4
9		1000	41.888	4+4

The planetary gearbox is filled with 1 l of a wind turbine gear oil with the physical and chemical properties described in the first part of the work [2].

4.1. Experimental results

Table 6 shows the test sequence and imposed input speed and torques. The tests were conducted at less than 50% of the load capacity of the planetary gearbox (low load).

Fig. 8 shows the stabilized operating temperatures in the planetary gearbox for the operating conditions presented in Table 6. The experimental results indicate that for a fixed speed and for a certain lubricant the stabilized operating temperature is almost constant. At these conditions the mineral based oil, MINR, has shown the overall lowest operating temperatures. MINE and PAOR performed identical and in between MINR and PAGD. PAGD has shown the highest operating temperatures specially as speed increases. The 300 rpm/750 N m test with MINR was disregarded since the temperature measurement was found faulty.

The power loss model was applied to the planetary gearbox. In this case, the model lacks the churning loss component, nevertheless some results are presented which allow us to draw some conclusions and explain the behaviour of the stabilized operating temperatures.

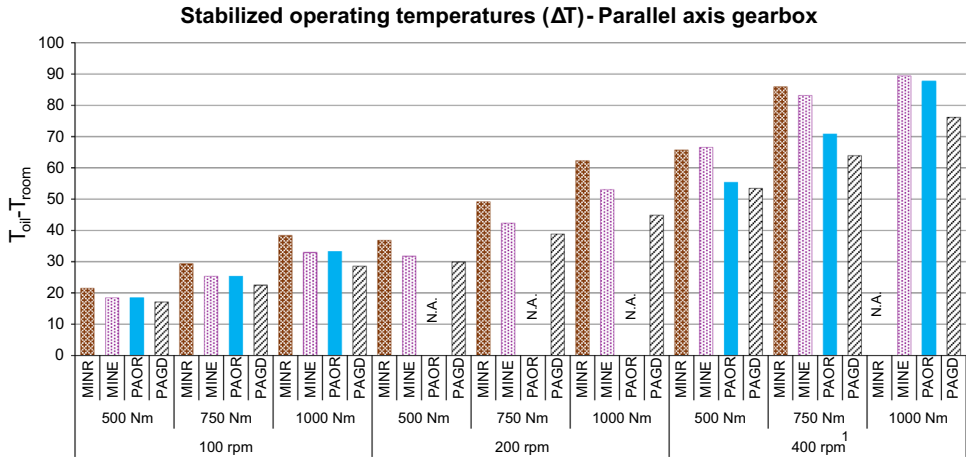

Fig. 3. Stabilized operating temperature. 1-MINE tests were performed at 500 instead of 400 rpm.

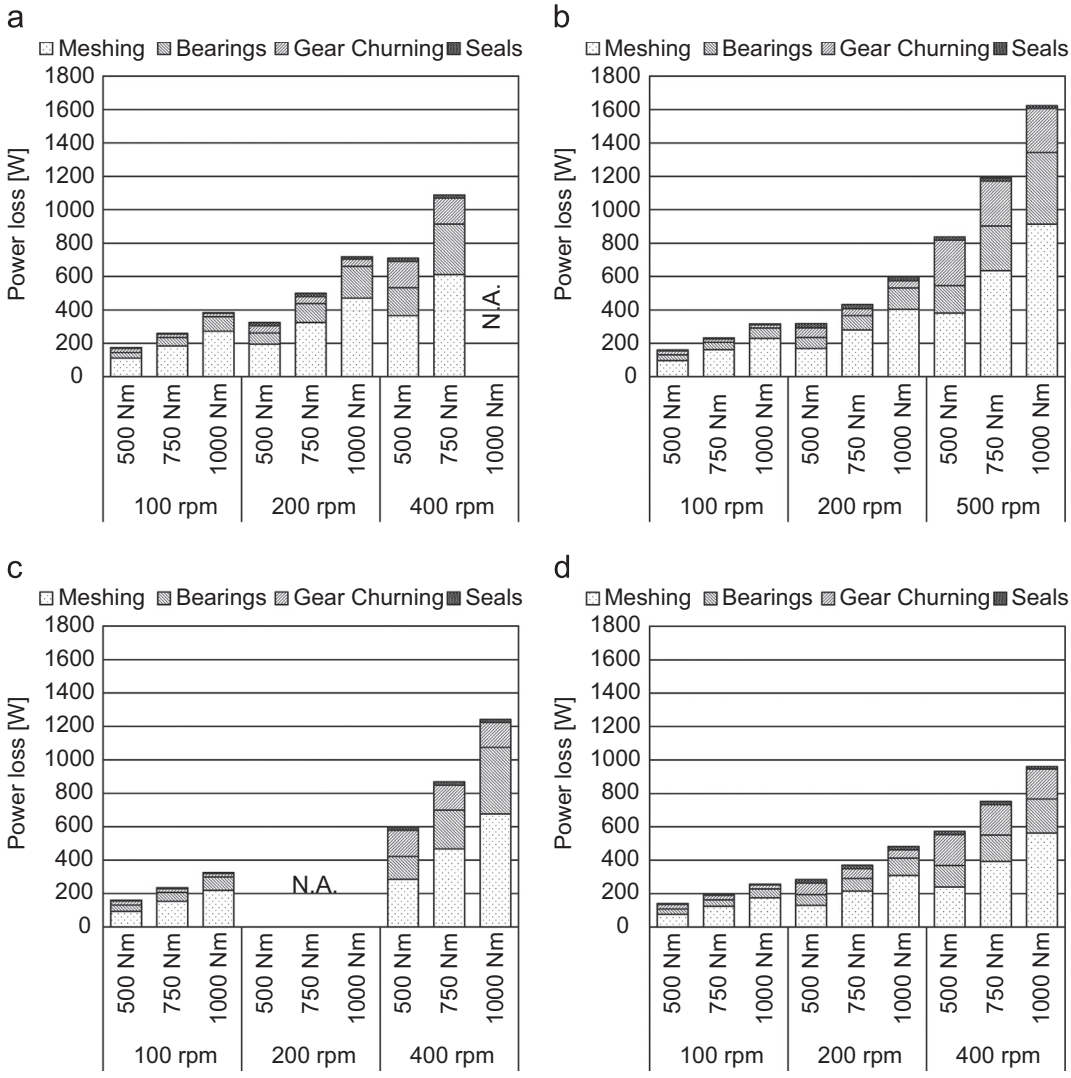

Fig. 4. Calculated power loss distribution for the parallel axis gearbox. (a) MINR, (b) MINE, (c) PAOR, (d) PAGD.

The stabilization temperature increases with increasing power, as expected.

4.2. Power loss modelling

The load dependant power loss model that was used to predict the power loss generated in the planetary gearbox is the same that was used in the calculations regarding the parallel axis gearbox. The model will be applied considering the power loss generated in the gearbox for the tested operating conditions for rolling bearings (Appendix A), gears (Appendix B) and seals (Appendix C).

4.2.1. Churning power loss in oil sump lubricated planetary gearboxes

As already referenced in a previous section, several authors presented works regarding the prediction of the power loss generated partly immersed gears. However in planetary gearboxes, the power loss generated by the air–oil mixture interaction with the moving mechanical elements has additional complications. The planet gears

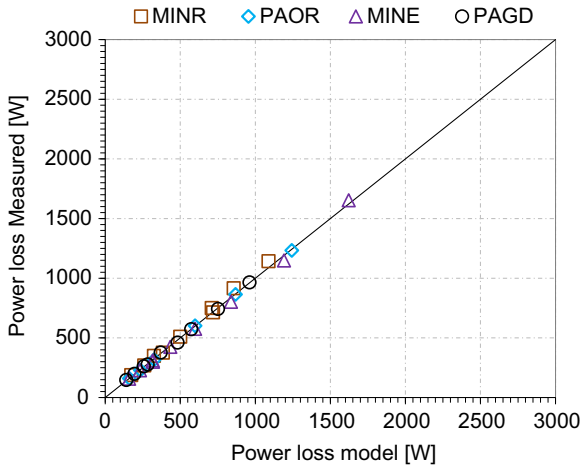

Fig. 5. Power loss measured vs. model simulations.

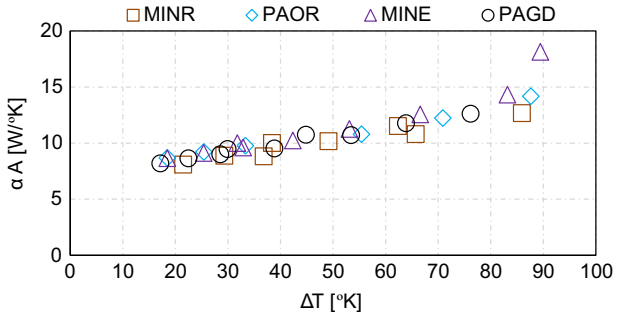

Fig. 6. Heat transfer coefficient calculated after the stabilized operating conditions and the predicted power loss.

Table 5
Rolling bearings in the planetary gearbox.

Bearing type	Quantity	Reference	Code	Lubrication
Tapered roller	2	32022 X/Q	B1,B2	Grease
Deep groove ball	1	6217-2Z	B3	Grease
Needle roller	6	K40 × 48 × 4	B4	Gear oil

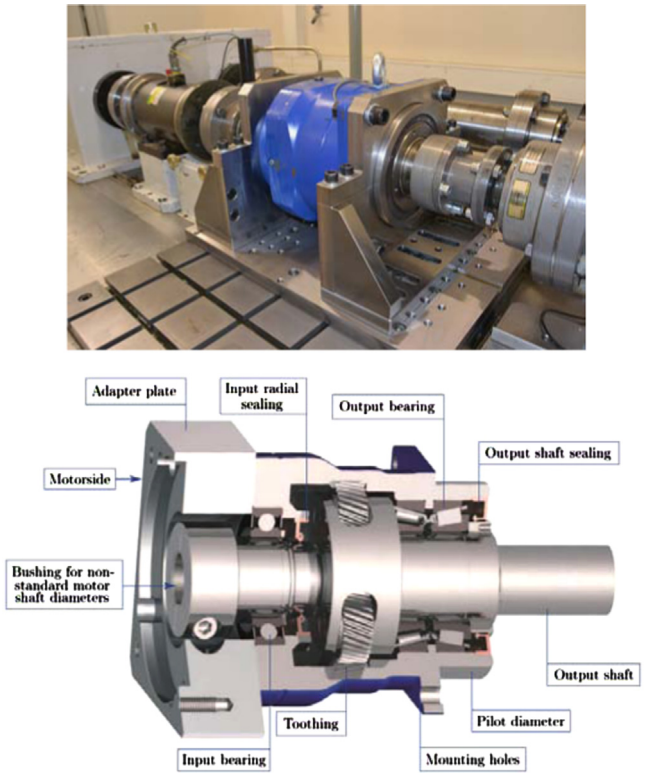

Fig. 7. Planetary gearbox installed in the test rig and schematic (reducer configuration).

Table 6
Sequence for the experimental tests (planetary gearbox).

Test sequence (–)	Input speed (rpm)	Input torque (N m)	Input power (kW)	Total test time (h)
1	100	500	5.236	2+2
2		750	7.854	2+2
3		1000	10.472	2+2
4	200	500	10.472	2+2
5		750	15.708	2+2
6		1000	20.944	2+2
7	300	500	15.707	2+2
8		750	23.562	2+2
9		1000	31.416	2+2

Table 4
Geometrical parameters of the gears in the planetary gearbox.

Gears				Parameters							
				z (–)	m (mm)	a (mm)	α (deg)	β (deg)	b (mm)	x (–)	Ra (μm)
Planetary	G1	Sun	36						−0.0189		
		Planet	36	2	74	20	10	42	−0.0189	0.4	
	G2	Ring	−108						+0.0566		

are animated with a rotational movement around their own centre combined with another rotational movement around the centre of the sun gear. The planet carrier is the element that holds the planet gears in place and allows the transport movement of the planets around the sun gear. In a planetary gearbox in oil sump lubrication several phenomena are prone to create power loss. Consider a planetary gearbox driven by the planet carrier but without the sun and internal gears. The result will be the planet carrier and the planets rotating as a single element. This movement alone is responsible for the majority of the power loss generated due to the air–oil mixture interaction with the moving elements. If the full planetary gearbox is considered, the power loss due to fluid trapping and squeezing as well as pumping effects due to the meshing gears must be considered. The rotation of the planets around its own centre can also create additional power loss.

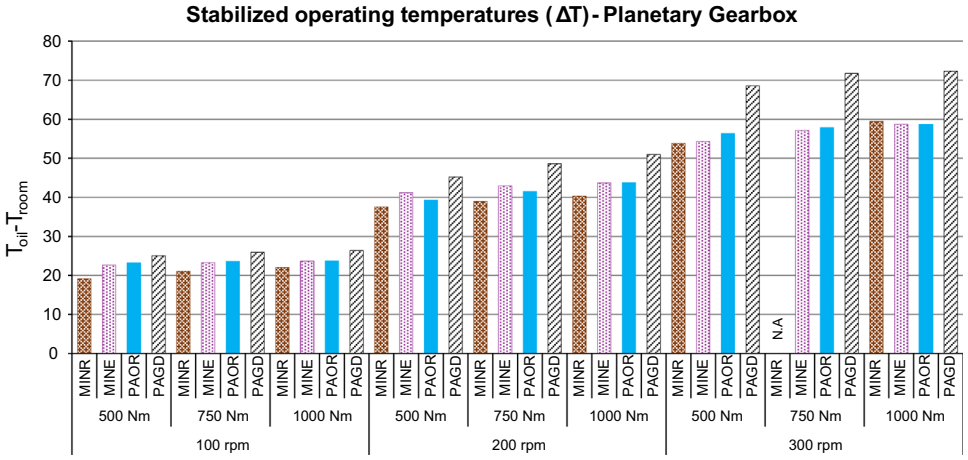

Fig. 8. Stabilized operating temperature.

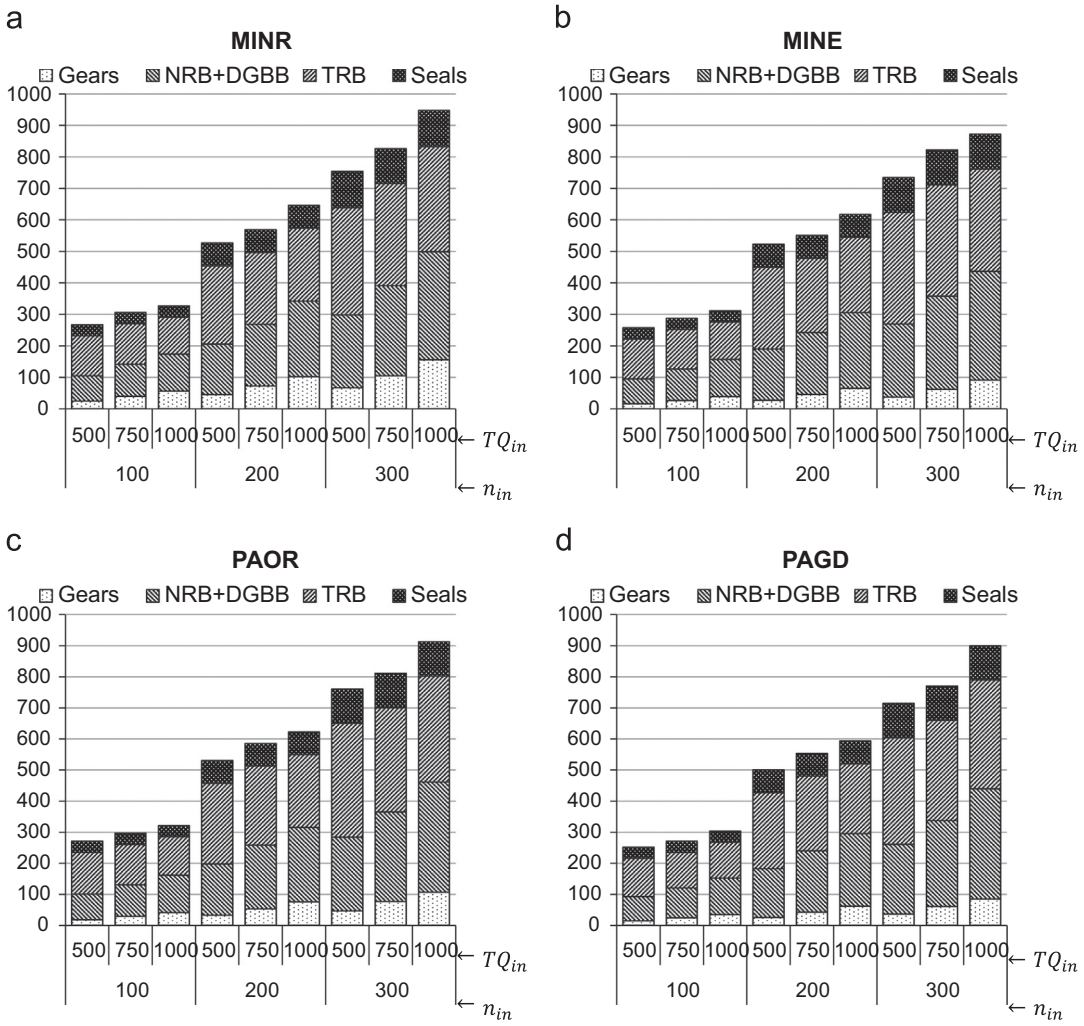

Fig. 9. Calculated power loss distribution for the planetary gearbox. (a) MINR, (b) MINE, (c) PAOR, (d) PAGD.

Recently Concli et al. [12] proposed a solution for the problem of the churning power loss in a planetary speed reducer which was based on a CFD approach.

4.3. Modelling results

The power loss model indicates that the power loss does not change that much with increasing torques (for a fixed speed), which is in agreement with the experimental results (Fig. 9). The model also suggests that all gear oils have similar power loss performance.

Fig. 9 shows the power loss behaviour of each individual power loss source in the planetary gearbox. The main power loss sources are the rolling bearings. The tapered roller bearings have a very high pre-load when compared to the axial forces introduced by the helical gears in the planetary gearbox, which results in approximately constant power loss for a certain operating speed. Since the tapered rolling bearings are the most important power loss source in the gearbox, the overall gearbox more or less follows their tendency.

The needle roller bearings are directly influenced by the input torque and speed, showing an almost direct correlation with the increase of the transmitted power.

None of the power loss sources that were considered seems to be able to explain the much higher operating temperature promoted by the PAGD oil. The only power loss component that was not considered was the churning loss. PAGD is the fluid with the highest density and viscosity index, which could have promoted higher churning power losses.

A calculation example can be found in Appendix D, for each power loss source of the planetary gearbox.

5. Conclusions

In this work the coefficients of friction derived from FZG tests were applied to a parallel axis and a planetary gearbox. The global heat transfer coefficient that was calculated after the stabilized operating temperatures and the predicted power loss shows that the model is consistent. Calculating the gears coefficient of friction from the results obtained in the FZG test rig seems to be an effective way to generate results that can be extended to a full gearbox allowing for a better understanding of the power loss behaviour of such mechanisms, when lubricated with different gear oils.

The experimental results (stabilized operating temperatures) indicate that changing the lubricating oil can have a severe impact in the power loss performance and operating temperature. Changing from MINR (mineral) to PAGD (polyalkylene glycol) in the parallel axis gearbox resulted in a reduction in power loss of $\approx 22\%$ and a much lower operating temperature. MINE and PAOR were in between MINR and PAGD.

The findings regarding the behaviour of the planetary contradict, in a sense, the results of the parallel axis gearbox. The characteristics of the internal gear mesh combined with the low load in each gear mesh resulted in very low gear mesh power losses. Due to the very high pre-load, the TRBs commanded the power loss behaviour of the planetary gearbox. By definition these tests were essentially conducted in almost no-load conditions. This explains the much higher operating temperatures generated by PAGD at the highest speed, which is the gear oil that has the highest density and the highest viscosity index.

Acknowledgements

The authors gratefully acknowledge the funding supported by: National Funds through *Fundação para a Ciência e a Tecnologia* (FCT), under the project EXCL/SEM-PRO/0103/2012; COMPETE and National Funds through *Fundação para a Ciência e a Tecnologia* (FCT), under the project Incentivo/EME/LA0022/2014; Quadro de Referência Estratégico Nacional (QREN), through Fundo Europeu de Desenvolvimento Regional (FEDER), under the project NORTE-07-0124-FEDER-000009 - Applied Mechanics and Product Development; without whom this work would not be possible.

Appendix A. Rolling bearings power loss

The new SKF model [13] considers that the total friction torque is the sum of four different physical sources of torque loss, represented by

$$M_t = M'_{rr} + M_{sl} + M_{drag} + M_{seal} \tag{A.1}$$

Eqs. (A.2) and (A.3) define the rolling and sliding torques, respectively,

$$M_{sl} = G_{sl} \cdot \mu_{sl} \tag{A.2}$$

$$M_{rr'} = \phi_{ish} \cdot \phi_{rs} \cdot [G_{rr}(n \cdot \upsilon)^{0,6}] \tag{A.3}$$

Eq. (A.4) defines the inlet shear heating and Eq. (A.5) shows the replenishment/starvation reduction factor:

$$\phi_{ish} = \frac{1}{1 + 1.84 \times 10^{-9} \cdot (n \cdot d_m)^{1.28} \cdot \nu^{0.64}} \tag{A.4}$$

$$\phi_{rs} = \frac{1}{e^{K_{rs} \cdot \nu \cdot n \cdot (d+D) \cdot \sqrt{K_z/2 \cdot (D-d)}}} \tag{A.5}$$

The rolling bearing drag losses' equations can be found in [13] for ball bearings or roller bearings. In the case of the grease lubricated rolling bearings of planetary gearbox studied, the drag losses should be disregarded.

The seal losses were not considered since the rolling bearings do not have seals.

The constants G_{sl}, G_{rr}, K_L, K_z and K_{rs} are dependent on the geometry of the rolling bearing.

The sliding friction torque (Eq. (A.6)) is dependent on the weighting factor (Eq. (A.7)) and on the reference values of the coefficient of friction (boundary film coefficient of friction – μ_{bl} and full-film coefficient of friction – μ_{EHD}) of each oil:

$$\mu_{sl} = \phi_{bl} \cdot \mu_{bl} + (1 - \phi_{bl}) \cdot \mu_{EHD} \tag{A.6}$$

$$\phi_{bl} = \frac{1}{e^{2,6 \times 10^{-8} (n \cdot \upsilon)^{1,4} \cdot d_m}} \tag{A.7}$$

The rolling bearing friction torque model, or torque loss model, only can predict accurate values if the boundary film coefficient of friction μ_{bl} and the full film coefficient of friction μ_{EHD} are

Table A1
Coefficient of friction of both TBB (ball element) and RTB (roller element) rolling bearings for an operating temperature of 80 °C [2].

Valid for: $3262.5 < n \cdot d_m < 52,200$			
Oil	Parameter	Bearing type	
		Ball element	Roller element
MINR	μ_{bl}	0.058	0.035
	μ_{EHD}	0.056	0.018
PAOR	μ_{bl}	0.049	0.039
	μ_{EHD}	0.044	0.010
MINE	μ_{bl}	0.044	0.044
	μ_{EHD}	0.027	0.008
PAGD	μ_{bl}	0.054	0.025
	μ_{EHD}	0.044	0.010

Table A2
Rolling bearing equations for SKF friction torque model.

Gearbox	Bearing reference	G_{rr}	G_{sl}
Parallel	RMS 11/RM 10/6307	$3.7\times10^{-7}\cdot d_m^{1.96}\cdot\left(F_r+\frac{1.7}{\sin\alpha_F}\cdot F_a\right)^{0.54}$	$2.84\times10^{-3}\cdot d_m^{-0.145}\cdot\left(F_r^5+\frac{92.8\cdot d_m^{1.5}}{\sin\alpha_F}\cdot F_a^4\right)^{1/3}$
	32306	$2.38\times10^{-6}\cdot d_m^{2.38}\cdot(F_r+10.9\cdot Y\cdot F_a)^{0.31}$	$0.019\cdot d_m^{0.82}\cdot(F_r+2\cdot Y\cdot F_a)$
	NJ 309E	$1.09\times10^{-6}\cdot d_m^{2.41}\cdot F_r^{0.31}$	$0.16\cdot d_m^{0.9}\cdot F_a+0.0015\cdot d_m\cdot F_r$
Planetary	32022 X/G	$2.38\times10^{-6}\cdot d_m^{2.38}\cdot(F_r+10.9\cdot Y\cdot F_a)^{0.31}$	$0.014\cdot d_m^{0.82}\cdot(F_r+2\cdot Y\cdot F_a)$
	6217-2Z	$3.9\times10^{-7}\cdot d_m^{1.96}\cdot\left(F_r+\frac{1.7}{\sin\alpha_F}\cdot F_a\right)^{0.54}$	$3.23\times10^{-3}\cdot d_m^{-0.145}\cdot\left(F_r^5+\frac{36.5\cdot d_m^{1.5}}{\sin\alpha_F}\cdot F_a^4\right)^{1/3}$

representative of the lubricant used and of the operating temperature of the rolling bearing. For mineral oils, whatever the rolling bearing element type, ball or roller, a value of $\mu_{bl}=0.15$ is suggested. Also for mineral oils a value of $\mu_{EHD}=0.05$ is proposed for ball element bearings, and a value of $\mu_{EHD}=0.02$ is proposed for roller element bearings [13].

There are no values of μ_{bl} and μ_{EHD} available for different gear oil formulations, neither for different operating temperatures. These values must be determined experimentally through rolling bearing tests. In part I of the present work [2], the values of μ_{bl} and μ_{EHD} were determined for different wind turbine gear oil formulations and are presented in Table A1.

The equations are resumed in Table A2 for each rolling bearing.

The axial load factor for the tapper roller bearings is $Y=1.4$.

The coefficient of friction determined in part I [2] for ball and roller bearings are not applicable for tapper roller bearings. In this case, the values suggested by SKF were used, i.e. $\mu_{bl}=0.15$ and $\mu_{EHD}=0.002$.

The frictional moment of the needle roller bearings, Eq. (A.8), was calculated according to Eschmann et al. [11,14] model.

In this model the torque loss in a rolling bearing is assumed to be the sum of the load (M_1) and no load (M_0) torque loss sources:

$$M_t^{NRB}=M_{VL0}+M_{VL1} \tag{A.8}$$

The frictional torque M_{VL0} results mainly from the lubricant friction, but also from the rolling element friction in the cage pockets and the cage friction at its guide surfaces. M_{VL0} depends predominantly on the operational viscosity of the lubricant, the speed, the design and size of the bearings.

The frictional torque M_{VL1} results mainly from the rolling friction, particularly from the hysteresis and friction effects. It hardly changes with the speed, but considerably with the rolling element pressure and therefore bearing load. It is additionally influenced by the design and size of the rolling bearing.

The rolling bearings power loss is given by

$$P_{VL}=M_t\cdot\omega \tag{A.9}$$

Appendix B. Meshing gears power loss

The meshing gears power loss is calculated using Ohlendorf's equation

$$P_{VZP}=P_{IN}\cdot H_V\cdot\mu_{mz} \tag{B.1}$$

The input power P_{IN} as given by the following equation:

$$P_{IN}=F_{bt}\cdot\omega\cdot r_b \tag{B.2}$$

Table B1
XL lubricant parameter.

Oil	X_L
MINR	0.846
PAOR	0.666
MINE	0.751
PAGD	0.585

Table C1
Seals dimensions.

Gearbox	Location	Code	d_{sh} (mm)
Parallel	Input shaft	S1	44.5
	Output shaft	S2	38
Planetary	Input shaft	S1	140
	Output shaft	S2	85

In the case of the planetary gearbox, the tangential force on the base plane is given by Eq. (B.3), where n_p is the number of planets:

$$F_{bt}=\frac{P_{IN}^g}{n_p\cdot v_t\cdot\cos\alpha} \tag{B.3}$$

The average coefficient of friction was determined using Schlenk's equation

$$\mu_{mZ}=0.048\cdot\left(\frac{F_{bt}/b}{\nu_{\Sigma C}\cdot\rho_{redC}}\right)^{0.2}\cdot\eta^{-0.05}\cdot R_a^{0.25}\cdot X_L \tag{B.4}$$

The lubricant factor X_L was determined in Part II of the present work [3]. Table B1 shows the adjusted lubricant factor for each one of the tested gear oils.

Appendix C. Seals power loss

The seal power loss was calculated using the below equation:

$$P_{VD}=7.69\times10^{-6}\cdot d_{sh}^2\cdot n \tag{C.1}$$

The seals shaft dimensions are presented in Table C1.

Appendix D. Calculation example

In order to clearly show the relative influence and the total influence of each gearbox element in the total power loss, the detailed result for the transfer gearbox is presented in Table D1. It

Table D1
Detailed power loss sources for a transfer gearbox operating at 200 rpm with 750 N m (MINR oil bath at 71.5 °C).

Element	Position	n_{in} (rpm)	Load		No-load		Total power loss
			$M_{sl} \cdot \omega$ (W)	$M_{sl} \cdot \omega$ (W)	$M_{drag} \cdot \omega$ (W)	P_{VL} (W)	P_V (W)
Rolling bearings	B1	196.1	32.9	3.9	0.02	36.8	111.7
	B2	196.1	1.7	0.6	0.001	2.2	
	B3	272.9	8.4	8.2	0.02	16.6	
	B4	272.9	22.3	12.2	0.02	34.5	
	B5	449.5	11.0	6.0	0.022	17.0	
	B6	449.5	2.8	1.9	0.01	4.6	
			μ_{mz}	P_{VZP} (W)	P_{VZ0} (W)	P_{VZ} (W)	
Gears	G1	196.1	0.051	136.8	42.9	179.7	409.5
G2	272.9	0.049	186.9			229.8	
					P_{VD} (W)	P_{VD} (W)	
Seals	S1	196.1	N.E.	N.E.	3.0	3.0	9.8
S2	449.5	N.E.	N.E.	6.8	6.8		

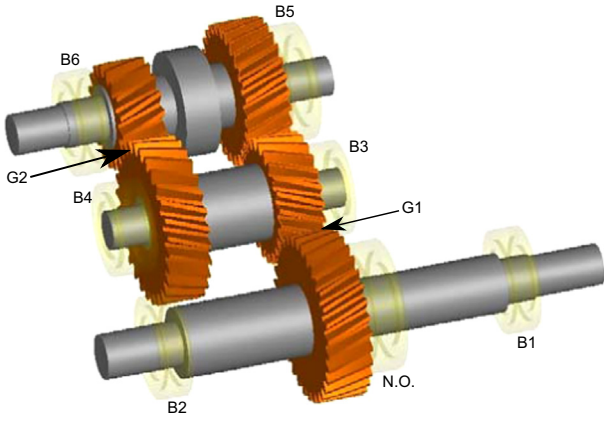

Fig. D1. Position of each gearbox element for the calculation example.

Table D2
Detailed power loss sources for a planetary gearbox operating at 200 rpm with 750 N m (MINR oil bath at 62.2 °C).

Element	Position	n_{in} (rpm)	Load		No-load		Total power loss
			$M_{sl} \cdot \omega$ (W)	$M_{sl} \cdot \omega$ (W)	$M_{drag} \cdot \omega$ (W)	P_{VL} (W)	P_V (W)
Rolling bearings	B1	195.4	2.1	135.0	0	137.1	310.0
	B2	195.4	2.0	133.5	0	135.5	
	B3	781.6	3.9	24.2	0	28.1	
	B4	195.4	5.4		3.9	9.3	
			μ_{mz}	P_{VZP} (W)	P_{VZ0} (W)	P_{VZ} (W)	
Gears	G1	195.4	0.0272	6.6	N.A.	$(3\times)6.6$	87.0
G2	195.4	0.0345	22.4			$(3\times)22.4$	
					P_{VD} (W)	P_{VD} (W)	
Seals	S1	195.4	N.E.	N.E.	29.4	29.4	72.8
S2	781.5	N.E.	N.E.	43.4	43.4		

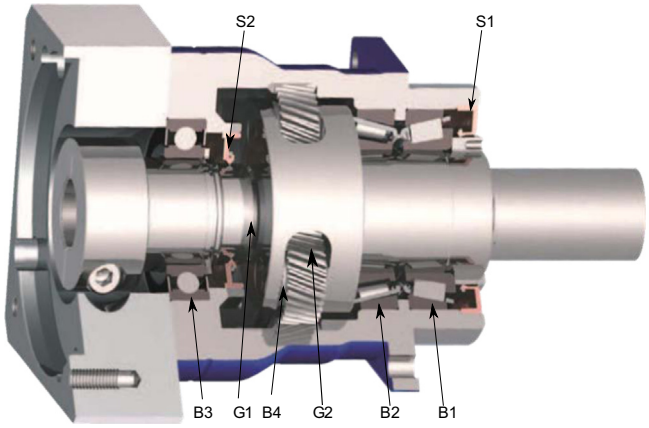

Fig. D2. Position of each planetary gearbox element for the calculation example.

was considered as example the gearbox tested under oil sump lubrication at 71.5 GC with a MINR oil with 200 rpm and 750 N m of applied load. Each element on the transfer gearbox is labelled according to Fig. D1.

For the planetary gearbox, it was considered as example the gearbox tested under oil sump lubrication at 62.2 GC with a MINR oil with 200 rpm and 750 N m of applied load. The results are detailed in Table D2. Each element on the planetary gearbox is labelled according to Fig. D2.

References

[1] Schlenk L. Untersuchungen zur Fresstragfähigkeit von Grossahnräedern [Ph.D. thesis]. Dissertation TU München; 1994.

[2] Fernandes C, Marques P, Martins R, Seabra J. Gearbox power loss. Part I: losses in rolling bearings. Tribol Int, http://dx.doi.org/10.1016/j.triboint.2014.11.017, in press.

[3] Fernandes C, Marques P, Martins R, Seabra J. Gearbox power loss. Part II: friction losses in gears. Tribol Int, http://dx.doi.org/10.1016/j.triboint.2014.12.004, in press.

[4] Marques PM, Fernandes CM, Martins RC, Seabra JH. Efficiency of a gearbox lubricated with wind turbine gear oils. Tribol Int 2014;71(0):7–16. http://dx.doi.org/10.1016/j.triboint.2013.10.017 URL ⟨http://www.sciencedirect.com/science/article/pii/S0301679X1300371X⟩.

[5] Changenet C, Leprince G, Ville F, Velex P. A note on flow regimes and churning loss modeling. J Mech Des 2011;133(12):121009. http://dx.doi.org/10.1115/1.4005330 URL ⟨http://link.aip.org/link/?JMD/133/121009/1⟩.

[6] Terekhov AS. Hydraulic losses in gearboxes with oil immersion. Vestn. Mashinostroeniya 1975;55(5):13–7.

[7] Lauster E, Boos M. Zum wärmehaushal mechanischer schaltgetriebe für nutzfahrzeuge. VDI-Ber 1983;488:45–55.

[8] Boness RJ. Churning losses of discs and gears running partially submerged in oil. In: Proceedings of ASME international power transmission gearing conference, vol. 1, 1989. p. 355–9.

[9] Höhn B-R, Michaelis K, Vollmer T. Thermal rating of gear drives: balance between power loss and heat dissipation. AGMA Technical Paper.

[10] Marques PM, Fernandes CM, Martins RC, Seabra JH. Power losses at low speed in a gearbox lubricated with wind turbine gear oils with special focus on churning losses. Tribol Int 2013;62:186–97. http://dx.doi.org/10.1016/j.triboint.2013.02.026 URL ⟨http://www.sciencedirect.com/science/article/pii/S0301679X13000777⟩.

[11] Höhn B-R, Michaelis K, Vollmer T. Thermal rating of gear drives: Balance between power loss and heat dissipation. AGMA Technical Paper.

[12] Concli F, Gorla C. Computational and experimental analysis of the churning power losses in an industrial planetary speed reducer. WIT Trans Eng Sci 2012;74:287–98.

[13] SKF General Catalogue 6000 EN, SKF, November 2005.

[14] Weigand EH. Ball and roller bearings—theory, design, and application. Munchen: Wiley; 1985.